Instrument Science Report COS 2019-16(v1)

Cycle 25 COS FUV Wavelength Scale Monitor

William J. Fischer[1]

[1] Space Telescope Science Institute, Baltimore, MD

7 August 2019

ABSTRACT

We report on the monitoring of the zero points of the COS FUV dispersion solutions during Cycle 25 in program 15385. Select cenwaves were monitored for all FUV gratings at Lifetime Position 4. All measured offsets are within the uncertainty thresholds of 6 pixels for G130M/1096, 3 pixels for the other G130M cenwaves, and 9 pixels for the G140L cenwaves.

Contents

Operated by the Association of Universities for Research in Astronomy, Inc., for the National Aeronautics and Space Administration.

1. Introduction

Analysis of data from thermal vacuum testing (TV03) indicates that grating-dependent offsets may develop in the dispersion solutions for the Cosmic Origins Spectrograph Far-Ultraviolet (COS FUV) channel (Oliveira et al. 2010). To determine whether any such changes are taking place, the COS FUV wavelength scale monitor obtains data annually for select cenwaves with gratings G130M, G160M, and G140L. The spectra are cross-correlated with COS spectra from the Cycle 22 iteration of this program and with FUSE or STIS data to measure any changes in the zero points of the dispersion solutions. The linear and, for G140L, quadratic terms in the solutions are not monitored.

We use a STIS E140M spectrum for comparison because of the superior wavelength accuracy of STIS relative to COS. The STIS E140M dispersion solutions have an absolute accuracy of 3.3 km s^{-1} (Riley et al. 2019). In contrast, the COS G130M and G160M dispersion solutions are accurate to 7.5 km s^{-1} (Plesha et al. 2019a), and the G140L dispersion solutions are accurate to 150 km s^{-1} (Fischer et al. 2019). The wavelength accuracy of FUSE is discussed by Dixon et al. (2007). It is accurate to 7 km s^{-1}, similar to the COS M modes. Point sources observed with FUSE through the LWRS aperture, the case for the spectrum discussed below, may suffer from a zero-point offset of up to 0.15 Å. We account for this possibility in the analysis.

2. Observations

The Cycle 25 FUV wavelength monitoring program (PID 15385, PI W. Fischer) consisted of one visit of three orbits to check the wavelength scales of the following gratings: G130M (cenwaves 1096, 1222, 1291, and 1327), G160M (cenwaves 1577 and 1623), and G140L (cenwaves 1105 and 1280). The target was AV 75, a star of spectral type O5.5I. Visit 01 successfully obtained the requisite data on 2018 March 12.

The acquisition sequence consisted of ACQ/SEARCH followed by ACQ/IMAGE using the Bright Object Aperture (BOA) and Mirror A. Because this is a crowded field, orients were put in place to avoid field objects that are too bright for the Primary Science Aperture (PSA) when the BOA is being used for acquisition. To mitigate the effects of gain sag, two FP-POS settings were used for each G130M and G160M cenwave, cycling among all four FP-POS throughout the visit. For G140L, only FP-POS 3 was used.

Due to the COS2025 rules designed to extend the lifetime of the FUV detector (Oliveira et al. 2018), the Cycle 25 program had some differences from its Cycle 24 predecessor (PID 14855, PI P. Sonnentrucker), which was described by Fischer (2018). In particular, the use of segment B is no longer supported for cenwave 1327. Implementing this restriction entailed moving the cenwave 1327 observations to the end of the visit, following cenwave 1105, which has always been used with only segment A. This reduces overhead, requiring segment B to be turned off only once. The exposures for the other cenwaves were then mildly rearranged to optimize use of the three orbits. Finally, the COS2025 rules required using FP-POS 3 for cenwave

Table 1. Settings Monitored in PID 15385

Grating	Cenwave	Segments	FP-POS	Total Time (s)
G130M	1096	BOTH	2, 4	1240
G130M	1222	BOTH	1, 3	452
G130M	1291	BOTH	3, 4	382
G130M	1327	FUVA	1, 3	384
G160M	1577	BOTH	2, 4	610
G160M	1623	BOTH	1, 3	738
G140L	1105	FUVA	3	80
G140L	1280	BOTH	3	80

1291 instead of the previous FP-POS 2. The monitored settings, segments, FP-POS, and exposure times are listed in Table 1. When two FP-POS are observed, the listed exposure time is split equally between them.

3. Analysis and Results

3.1 Window Selection

The cross-correlation analysis was performed in distinct windows featuring absorption lines formed along the line of sight to the target. The windows have been revised from those used in the reports of previous cycles. Those used for the medium-resolution cenwaves are listed in Table 2. Below 1090 Å, they were selected with the aid of a FUSE spectrum of AV 75 (PID P115, PI J. M. Shull). Above 1090 Å, windows were based on those used for the recent improvements to the dispersion solutions of the G130M and G160M modes (Plesha et al. 2019a; P2019 in Table 2). Above 1300 Å, this list is fairly sparse, so we added select windows used for the analysis of dispersion solutions by Sonnentrucker et al. (2013; S2013 in Table 2). For the low-resolution cenwaves, we evaluated the suitability of each medium-resolution window and selected a subset for use, widening and combining them if necessary to accommodate the broader lines. These are listed in Table 3. Each monitored segment contains between three and fourteen windows, with the number typically decreasing toward longer wavelengths.

3.2 Comparison to Previous COS Spectra

The first part of the analysis was to cross-correlate the new COS spectra with those obtained in previous iterations of this program. The lifetime position (LP) at which the spectra are acquired is relevant, because each has its own wavelength calibration.

Table 2. Medium-Resolution Cross-Correlation Windows

Minimum (Å)	Maximum (Å)	Source	Minimum (Å)	Maximum (Å)	Source
946.0	948.2	FUSE	1239.5	1241.7	P2019
1012.0	1016.0	FUSE	1249.7	1252.0	P2019
1043.2	1045.4	FUSE	1252.9	1255.6	P2019
1049.0	1052.3	FUSE	1258.0	1263.0	P2019
1062.0	1065.7	FUSE	1263.8	1266.5	P2019
1076.5	1078.5	FUSE	1276.0	1279.0	P2019
1078.8	1080.2	FUSE	1301.7	1303.6	S2013
1093.0	1093.5	P2019	1303.8	1305.8	S2013
1093.8	1095.0	P2019	1333.0	1337.5	P2019
1096.7	1097.7	P2019	1369.5	1371.5	P2019
1107.8	1109.4	P2019	1393.3	1395.0	S2013
1109.9	1110.8	P2019	1402.3	1404.3	S2013
1111.9	1112.8	P2019	1525.0	1529.5	P2019
1112.8	1113.3	P2019	1559.8	1560.7	P2019
1116.0	1116.8	P2019	1607.0	1610.5	P2019
1125.1	1126.3	P2019	1611.0	1613.0	P2019
1152.0	1154.0	P2019	1655.5	1659.0	P2019
1189.8	1192.0	P2019	1670.4	1671.1	S2013
1192.7	1194.7	P2019	1741.8	1742.6	S2013

Table 3. Low-Resolution Cross-Correlation Windows

Minimum (Å)	Maximum (Å)	Minimum (Å)	Maximum (Å)
945.5	952.5	1249.0	1256.0
1060.0	1066.0	1257.5	1264.0
1076.0	1084.0	1333.0	1337.5
1091.0	1096.0	1524.5	1529.5
1106.0	1114.5	1607.0	1613.0
1187.0	1196.0	1668.0	1673.0

(The LP refers to the detector region on which COS spectra fall, which is updated every few years to mitigate the effects of declining gain.) AV 75 has been used as a wavelength monitoring target since Cycle 20 (2013), when LP2 was in use for all cenwaves. G130M/1096 spectra have continued to be acquired at LP2, while those for all other monitored cenwaves were acquired at LP2 in Cycle 21 (2014), at LP3 in Cycles 22 through 24 (2015–2017), and at LP4 in Cycle 25 (2018).

Recently the wavelength solutions for most of the G130M and G160M cenwaves were improved. They are now accurate to 7.5 km s^{-1} instead of the original 15 km s^{-1}. Of the cenwaves monitored here, G130M/1291, G130M/1327, G160M/1577, and G160M/1623 were updated at LP2 (Ake et al. 2019), and all of these cenwaves plus G130M/1222 were updated at LP3 and LP4 (Plesha et al. 2019b,a).

To monitor the long-term stability of the zero points, we compare COS spectra to those obtained in the Cycle 22 instance of this program, the first to take place at LP3, because the updating of the dispersion solutions is less complete in earlier datasets. As a consequence of LP3 commissioning, these spectra were obtained in two programs that ran five days apart (PIDs 13931 and 13969, PIs J. Roman-Duval and P. Sonnentrucker, respectively). The results of the Cycle 25 COS-COS analysis appear in Table 4. In all tables and figures, the reported shifts are the medians of those measured in all windows considered for each segment.

The same analysis was also performed for Cycles 20 through 24, and the shifts for all cycles are plotted in Figure 1. Those for Cycle 22 (2015) are zero by definition, since it is the basis for comparison. The dashed lines in each panel show the error goals. These are 6 pixels for G130M/1096 because its solution was not recently updated, 3 pixels for the other medium-resolution modes, and 9 pixels (150 km s^{-1} at 1450 Å) for G140L.

All shifts are within the error goals. The LP2 (2014) data for G130M/1222 have atypically large shifts because the LP2 solutions were not updated in the recent effort. There is evidence for a slight trend toward more negative shifts for some modes in recent iterations of the program. We will continue monitoring this in upcoming cycles to determine whether it is significant.

3.3 Comparison to FUSE and STIS Spectra

The second part of the analysis was to cross-correlate the new COS spectra with FUSE and STIS spectra of AV 75. The FUSE spectrum is the one mentioned above for window selection. For STIS we use an E140M spectrum acquired in Cycle 7 (PID 7437, PI D. Lennon). We cross-correlated the FUSE spectrum with the STIS spectrum in the region where they overlap and found that the FUSE spectrum is shifted to shorter wavelengths by 0.0106 Å. The FUSE wavelength scale was corrected by this offset, which corresponds to 1.06 pixels for the COS M modes and 0.13 pixels for the COS L modes. The results of the Cycle 25 analysis appear in Table 5.

The same analysis was also performed for Cycles 20 through 24, and the shifts for all cycles are plotted in Figure 2. The dashed lines in each panel show the same

Table 4. Pixel Shifts from COS-COS Cross-Correlation (Cycle 25 vs. Cycle 22)[1]

Seg.	G130M 1096	G130M 1222	G130M 1291	G130M 1327	G160M 1577	G160M 1623	G140L 1105	G140L 1280
A	−0.4	−1.0	−0.4	−0.3	−2.6	−2.3	−1.0	−0.3
B	−0.5	−1.3	−0.4	··· [2]	−1.6	−2.3	··· [2]	−0.1

[1]Shifts are those required to bring the Cycle 25 data into agreement with the Cycle 22 data.

[2]Data are not collected at this setting.

Table 5. Pixel Shifts from COS-FUSE/STIS Cross-Correlation[1]

Seg.	G130M 1096	G130M 1222	G130M 1291	G130M 1327	G160M 1577	G160M 1623	G140L 1105	G140L 1280
A	−3.6	+0.2	−0.3	+0.2	−0.1	··· [2]	−3.8	−1.4
B	+4.9	−0.3	+0.5	··· [3]	−0.7	+0.2	··· [3]	−3.2

[1]Shifts are those required to bring the COS data into agreement with the FUSE data (for G130M/1096, G130M/1222/B, and G140L/1280/B) or STIS data (all other settings).

[2]No FUSE or STIS data are available for this setting.

[3]Data are not collected at this setting.

error goals as before; all shifts are within them. For the modes with updated dispersion solutions, recent spectra have excellent agreement with spectra from other instruments. For modes that were not updated (G130M/1096 and both G140L cenwaves), there are persistent offsets of a few pixels, but the shifts are still within the specifications.

4. Continuation Plan

This program continues in Cycle 26 as PID 15536 and is identical to the Cycle 25 version.

Change History for COS ISR 2019-16

Version 1: 7 August 2019 – Original Document

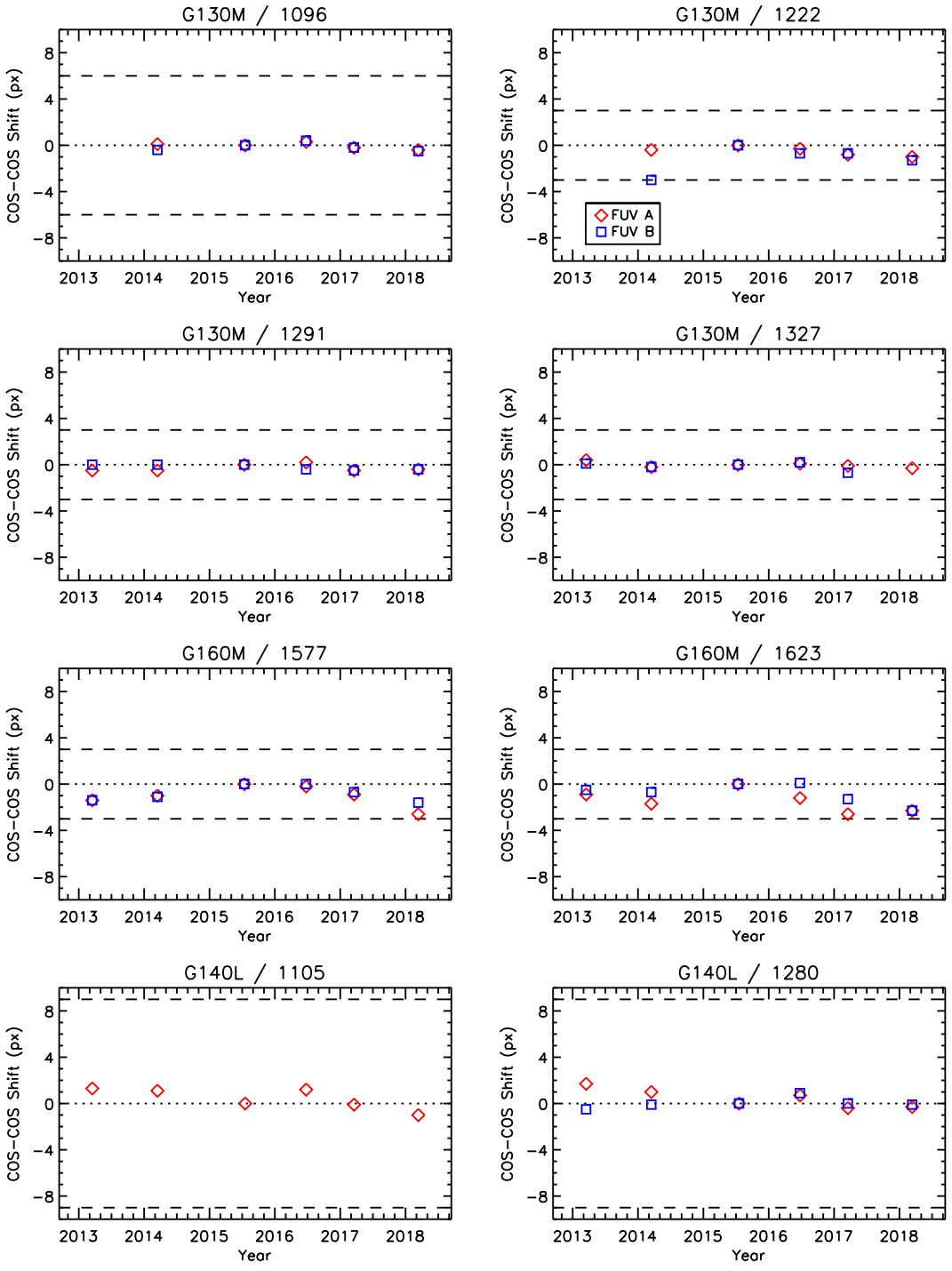

Figure 1. Plots of COS-COS shifts for the eight cenwaves monitored with AV 75 since Cycle 21 (2014) or before. Shifts are those required to bring each spectrum into agreement with the Cycle 22 data. Symbol types distinguish between segments. Dashed lines indicate the error goals.

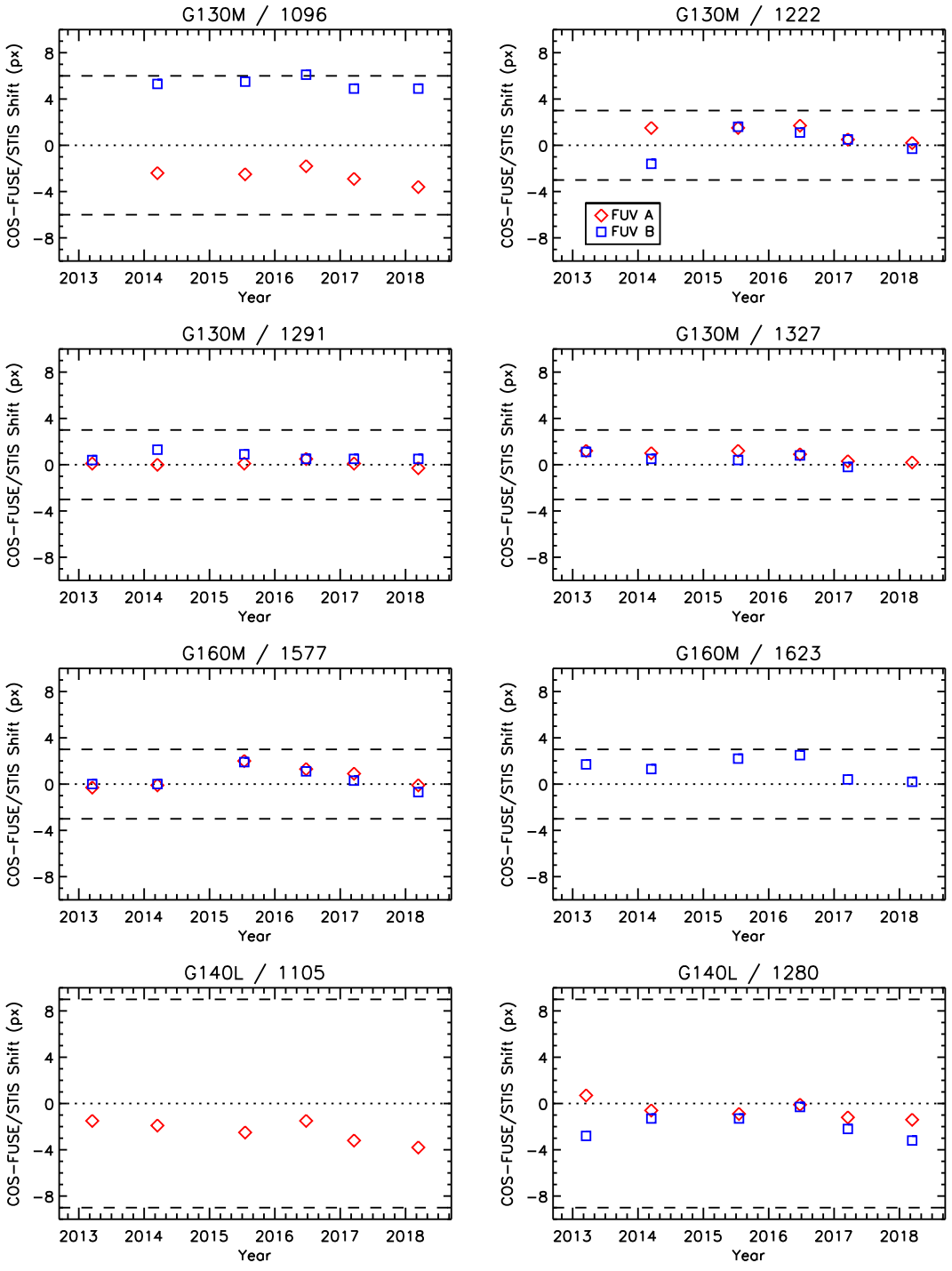

Figure 2. Plots of COS-FUSE/STIS shifts for the eight cenwaves monitored with AV 75 since Cycle 21 (2014) or before. Shifts are those required to bring each COS spectrum into agreement with the FUSE or STIS data. Symbol types distinguish between segments. Dashed lines indicate the error goals.

References

Ake, T., Plesha, R., De Rosa, G., et al. 2019, COS ISR 2018-23, "Improvements to the COS FUV G130M and G160M Wavelength Solutions at Lifetime Position 2"

Dixon, W. V., Sahnow, D. J., Barrett, P. E., et al. 2007, PASP, 119, 527

Fischer, W. J. 2018, COS ISR 2018-06, "Cycle 24 COS FUV Internal/External Wavelength Scale Monitor"

Fischer, W. J., et al. 2019, *Cosmic Origins Spectrograph Instrument Handbook*, Version 11.0 (Baltimore: STScI)

Oliveira, C., Béland, S., Keyes, C., & Niemi, S. 2010, COS ISR 2010-06, "SMOV: COS FUV Wavelength Calibration"

Oliveira, C., De Rosa, G., Mackenty, J., et al. 2018, COS ISR 2018-16, "COS2025: A New Strategy to Prolong the Lifetime of the COS/FUV Detector to 2025"

Plesha, R., Ake, T., De Rosa, G., Oliveira, C., & Penton, S. 2019a, COS ISR 2018-25, "Improvements to the COS FUV G130M and G160M Wavelength Solutions at Lifetime Position 4"

Plesha, R., Ake, T., De Rosa, G., Oliveira, C., & Penton, S. 2019b, COS ISR 2018-24, "Improvements to the COS FUV G130M and G160M Wavelength Solutions at Lifetime Position 3"

Riley, A., et al. 2019, *Space Telescope Imaging Spectrograph Instrument Handbook*, Version 18.0 (Baltimore: STScI)

Sonnentrucker, P., Roman-Duval, J., Ely, J., et al. 2013, COS ISR 2013-06, "COS FUV Dispersion Solution Verification at the New Lifetime Position"